

RAPID REPORT

Kinetics of Mg^{2+} unblock of NMDA receptors: implications for spike-timing dependent synaptic plasticity

Björn M. Kampa^{1,2}, John Clements¹, Peter Jonas² and Greg J. Stuart^{1,2}

¹Division of Neuroscience, John Curtin School of Medical Research, Australian National University, Canberra, Australia

²Physiology Institute I, University of Freiburg, Freiburg, Germany

The time course of Mg^{2+} block and unblock of NMDA receptors (NMDARs) determines the extent they are activated by depolarization. Here, we directly measure the rate of NMDAR channel opening in response to depolarizations at different times after brief (1 ms) and sustained (4.6 s) applications of glutamate to nucleated patches from neocortical pyramidal neurons. The kinetics of Mg^{2+} unblock were found to be non-instantaneous and complex, consisting of a prominent fast component (time constant $\sim 100 \mu s$) and slower components (time constants 4 and ~ 300 ms), the relative amplitudes of which depended on the timing of the depolarizing pulse. Fitting a kinetic model to these data indicated that Mg^{2+} not only blocks the NMDAR channel, but reduces both the open probability and affinity for glutamate, while enhancing desensitization. These effects slow the rate of NMDAR channel opening in response to depolarization in a time-dependent manner such that the slower components of Mg^{2+} unblock are enhanced during depolarizations at later times after glutamate application. One physiological consequence of this is that brief depolarizations occurring earlier in time after glutamate application are better able to open NMDAR channels. This finding has important implications for spike-timing-dependent synaptic plasticity (STDP), where the precise (millisecond) timing of action potentials relative to synaptic inputs determines the magnitude and sign of changes in synaptic strength. Indeed, we find that STDP timing curves of NMDAR channel activation elicited by realistic dendritic action potential waveforms are narrower than expected assuming instantaneous Mg^{2+} unblock, indicating that slow Mg^{2+} unblock of NMDAR channels makes the STDP timing window more precise.

(Received 28 November 2003; accepted after revision 28 January 2004; first published online 30 January 2004)

Corresponding author G. Stuart: Division of Neuroscience, John Curtin School of Medical Research, Australian National University, Canberra, Australia. Email: Greg.Stuart@anu.edu.au

Excitatory synaptic transmission at vertebrate central synapses is mediated primarily by the neurotransmitter glutamate. The resulting postsynaptic current typically consists of a fast component mediated by AMPA receptors and a slow component mediated by NMDARs (Forsythe & Westbrook, 1988; Bekkers & Stevens, 1989). Current flow through NMDAR channels is largely blocked by external Mg^{2+} ions at resting membrane potentials, but can be relieved by depolarization (Mayer *et al.* 1984; Nowak *et al.* 1984). The voltage-dependent block and unblock of NMDAR channels by Mg^{2+} is thought to be extremely rapid (Jahr & Stevens, 1990*a,b*), and is usually assumed to be effectively instantaneous. A recent study, however, indicates there is a slow component to Mg^{2+} unblock of NMDAR channels (Vargas-Caballero &

Robinson, 2003), which may have important physiological implications.

NMDARs receptors play a key role in the induction of many forms of synaptic plasticity (Bliss & Collingridge, 1993). As NMDARs are largely blocked by Mg^{2+} at resting membrane potentials, the kinetics of Mg^{2+} unblock of NMDAR channels will influence NMDAR activation during synaptic plasticity induction. This is likely to be particularly important during spike-timing dependent plasticity (STDP), where the coincidence of EPSPs and action potentials (APs) within a brief time window determines the magnitude and sign of changes in synaptic strength (Markram *et al.* 1997; Bi & Poo, 1998). In cortical pyramidal neurons APs are brief events which attenuate as they propagate back into the dendritic tree (Stuart

et al. 1997). Hence, the ability of backpropagating APs to activate synaptic NMDARs, and so control calcium influx through the NMDAR channel, will be critically dependent on the time course of Mg^{2+} unblock. Here, we directly investigate the kinetics and time dependence of Mg^{2+} unblock of NMDARs during rapid applications of glutamate to nucleated patches from cortical layer 5 pyramidal neurons. In addition, we provide a kinetic model that can explain our findings.

Methods

Wistar rats (2–4 weeks old) were anaesthetized by inhalation of isoflurane, decapitated, and sagittal brain slices (300 μ m) of somatosensory cortex were prepared according to guidelines approved by the Animal Ethics Committee of the Australian National University and the University of Freiburg. During recording, slices were superfused with oxygenated extracellular solution containing 125 mM NaCl, 3 mM KCl, 1.25 mM NaH_2PO_4 , 25 mM $NaHCO_3$, 25 mM glucose, 2 mM $CaCl_2$, 1 mM $MgCl_2$ (pH 7.4 with 5% CO_2). Nucleated patch experiments were performed at room temperature ($\sim 23^\circ C$) using pipettes filled with 137 mM CsCl, 4 mM $MgCl_2$, 10 mM Hepes, 10 mM EGTA, 4 mM Na_2ATP , 10 mM Na_2 -phosphocreatine (pH 7.2 with CsOH) or in some cases with 80 mM CsCl, 80 mM CsF, 4 mM Na_2ATP , 2 mM $MgCl_2$ (pH 7.2 with CsOH). Gigaseals (5–10 G Ω) were formed onto the soma of layer 5 pyramidal neurons with patch pipettes (resistance 3–5 M Ω) using a patch-clamp amplifier (AxoPatch 200A; Axon Instruments). After obtaining the whole-cell configuration negative pressure was applied to the recording pipette and the nucleus with the surrounding cell membrane was pulled out of the slice to obtain a nucleated patch (Sather *et al.* 1992). The solution around nucleated patches was changed rapidly using a two-barrel application pipette attached to a piezo-electric device (Colquhoun *et al.* 1992). Nucleated patches were superfused with Hepes-buffered extracellular solution containing 125 mM NaCl, 10 mM Hepes, 3 mM KCl, 2 mM $CaCl_2$, 1 mM $MgCl_2$, 20 μ M DNQX, 10 μ M glycine, 200 μ M $CdCl_2$, 0.1 μ M TTX (pH 7.4 with NaOH) and for the times indicated switched to the same solution containing 1 mM L-glutamate. Traces were recorded with and without glutamate application for subtraction of leak and capacitance currents and averaged. Open tip responses during brief (1 ms) and long (4.6 s) changes into and out of diluted (10%) Hepes-buffered extracellular solution were checked before each experiment (20–80% rise time ~ 200 μ S). For the kinetic model (Fig. 2), and during pairing of glutamate applications with voltage

commands obtained during dendritic recordings (Fig. 4), the timing of glutamate applications was corrected for the delay (~ 2 ms) required for the glutamate solution to reach the patch following activation of the piezo-electric device. The holding potential during action potential waveforms (-66 mV, Fig. 4A) was corrected for the difference in junction potential between the potassium gluconate- and CsCl-based recording solutions (-9 mV). Glutamate-activated currents were hardware filtered at 5 kHz (8-pole Bessel; Axopatch 200A) and sampled at 50 kHz on a Macintosh computer. AxoGraph software (Axon Instruments) was used for both acquisition and analysis. Statistical significance was tested with the Students *t* test ($\alpha = 0.05$) and pooled data shows mean \pm s.e.m. For display purposes current traces in the figures were digitally filtered at 1 kHz.

Recorded NMDAR currents were fitted using a 10-state Markov model of the NMDAR, five states with Mg^{2+} bound and five unbound states (Fig. 2A). Reaction rates between the states were adjusted until the best fit to the data was obtained. Modelling and fitting were performed using AxoGraph 4.9 (Axon Instruments), which employs a simplex algorithm to minimize the sum of squared errors between simulated traces and data. The model incorporated several simplifications and constraints to keep the number of free parameters manageable. Only a single glutamate binding step was included as binding is effectively instantaneous at 1 mM. The binding rate was constrained to 10 μ M $^{-1}$ s $^{-1}$ based on previous estimates (Clements & Westbrook, 1991). As the NMDAR channel opening rate is low (Rosenmund *et al.* 1995), and has negligible influence on the kinetic properties of the receptor, this was arbitrarily constrained to 10 s $^{-1}$. The data contain no information about the Mg^{2+} binding rate, and this was constrained to 0.05 μ M $^{-1}$ s $^{-1}$ for Mg^{2+} binding to the open state at +40 mV based on previous estimates (Ascher *et al.* 1988; Jahr & Stevens, 1990*a,b*). Mg^{2+} binding to the other four states was arbitrarily constrained to be 1000 times slower. The voltage dependence of the Mg^{2+} binding and unbinding rates is determined by the Mg^{2+} ion valency (2) and the position of the Mg^{2+} binding site 80% of the way from the extracellular side through the membrane field (Jahr & Stevens, 1990*a*). Mg^{2+} concentration was set to 1 mM. As the time course of desensitization during long pulses was double exponential, two desensitized states were required. The model contains four reaction cycles, so four of the rates were constrained by cyclic reversibility. The fitting process started by fitting data recorded at +40 mV with a five-state model that excluded Mg^{2+} bound states. The optimum rates obtained were then constrained in the subsequent fit of the full 10-state

model to the data incorporating voltage steps from -60 to +40 mV (Fig. 2B). The microscopic K_d for glutamate binding was calculated as unbinding rate/binding rate, open probability was calculated as opening rate/(opening

rate + closing rate), and percentage desensitization was calculated as desensitization rate/(desensitization rate + re-sensitization rate). Changes in microscopic K_d are unlikely to be due to changes in glycine affinity as the

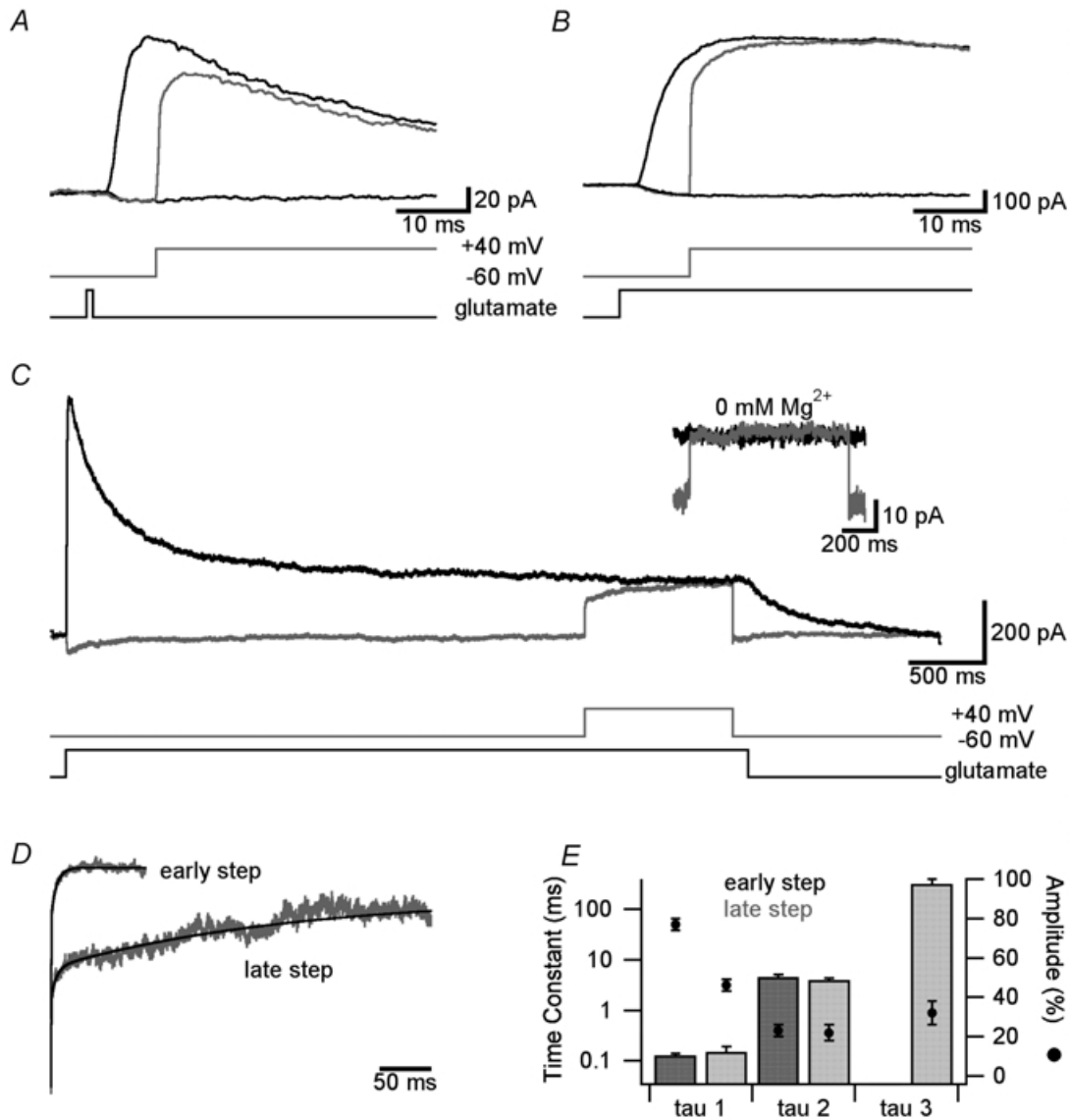


Figure 1. The magnitude of slow unblock depends on the timing of depolarization

A, superimposed NMDAR currents during 1 ms applications of 1 mM glutamate in the presence of 1 mM Mg²⁺ at holding potentials of -60 and +40 mV (black), and during a step from -60 to +40 mV starting 10 ms after glutamate application (grey). The timing of glutamate application and the voltage step from -60 to +40 mV are indicated at the bottom. B, same as in A but during a long (4.6 s) application of glutamate. C, same as A and B during a 1 s voltage step from -60 to +40 mV starting 3.5 s after a long (4.6 s) application of 1 mM glutamate (grey). Inset shows same voltage step applied to a different patch in solution without external Mg²⁺. D, NMDAR current at +40 mV divided by that during steps from -60 to +40 mV starting 10 ms ('early step'; data from B) or 3.5 s ('late step'; data from C) after long (4.6 s) applications of 1 mM glutamate. Black traces show multiexponential fits. E, pooled data ($n = 5$) of the time constant (columns) and relative amplitude (●) of multiexponential fits to Mg²⁺ unblock during steps from -60 to +40 mV starting 10 ms ('early step'; dark grey) and 3.5 s ('late step'; light grey) after long applications of glutamate. Steps at 10 ms were fitted with a double exponential, whereas a triple exponential was required to fit steps at 3.5 s.

concentration of glycine used in our experiments ($10 \mu\text{M}$) is approximately 100 times the apparent K_d (Johnson & Ascher, 1992).

Simultaneous somatic and dendritic recordings were made from the soma and apical dendrite of layer 5 pyramidal neurons as previously described (Stuart *et al.* 1997) using current-clamp amplifiers (Dagan), hardware filtered at 10 kHz and sampled at 50 kHz on a Macintosh computer. Recordings were made at 35°C using pipettes filled with 135 mM potassium gluconate, 7 mM NaCl, 10 mM Hepes, 2 mM MgCl_2 , 2 mM Na_2ATP (pH 7.2 with KOH). EPSPs were evoked by extracellular stimulation with a patch pipette filled with external solution placed approximately $20 \mu\text{m}$ from the dendritic recording site, and APs were evoked by brief (2 ms) somatic current injections (3 nA).

Results

NMDAR currents were evoked in nucleated patches from neocortical layer 5 pyramidal neurons by brief (1 ms) glutamate pulses to mimic the synaptic release of glutamate (Clements *et al.* 1992; Colquhoun *et al.* 1992). Currents recorded at a holding potential of $+40 \text{ mV}$ to prevent Mg^{2+} block had an average amplitude of $189 \pm 29 \text{ pA}$, a rise time constant of $2.0 \pm 0.2 \text{ ms}$ and decayed in a double exponential manner with time constants of $32 \pm 1.5 \text{ ms}$ (amplitude: $51 \pm 1.6\%$) and $176 \pm 17.2 \text{ ms}$ (amplitude: $49 \pm 1.6\%$; $n = 12$). In the presence of physiological concentrations of external Mg^{2+} (1 mM) NMDAR currents were largely blocked at -60 mV (Fig. 1A). Stepping the holding potential from -60 to $+40 \text{ mV}$ starting 10 ms after onset of glutamate application resulted in a reversal of the inward current at -60 mV towards the outward current obtained during application of glutamate at $+40 \text{ mV}$ (Fig. 1A). However, the NMDAR current did not instantaneously reach that observed during glutamate application at $+40 \text{ mV}$, but showed a slow component (Fig. 1A). Similar results were observed when glutamate was applied throughout the duration of depolarizing voltage steps from -60 to $+40 \text{ mV}$ (Fig. 1B). In Mg^{2+} -free solutions the current reversed instantaneously during depolarizations from -60 to $+40 \text{ mV}$ (time constant of $0.07 \pm 0.01 \text{ ms}$, $n = 5$), indicating that the slow time course of current reversal was due to slow unblock by Mg^{2+} (see Fig. 1C, inset). The ratio of the current evoked at $+40 \text{ mV}$ and that evoked by stepping from -60 to $+40 \text{ mV}$ starting 10 ms after onset of glutamate application was used to assess the rate of Mg^{2+} unblock (Fig. 1D; 'early step'). After brief (1 ms) glutamate applications this current ratio was best fitted with two exponentials with average

time constants of $0.13 \pm 0.02 \text{ ms}$ and $3.1 \pm 0.7 \text{ ms}$ and relative amplitudes of $68 \pm 3\%$ and $32 \pm 3\%$, respectively ($n = 7$). A similar time course of Mg^{2+} unblock was observed when glutamate was applied throughout the duration of these depolarizations (Fig. 1E and $0.13 \pm 0.01 \text{ ms}$ and $4.6 \pm 0.5 \text{ ms}$ with relative amplitudes of $77 \pm 3\%$ and $23 \pm 3\%$, respectively; $n = 5$).

To investigate the dependence of this slow Mg^{2+} unblock on the timing of the depolarization we also applied

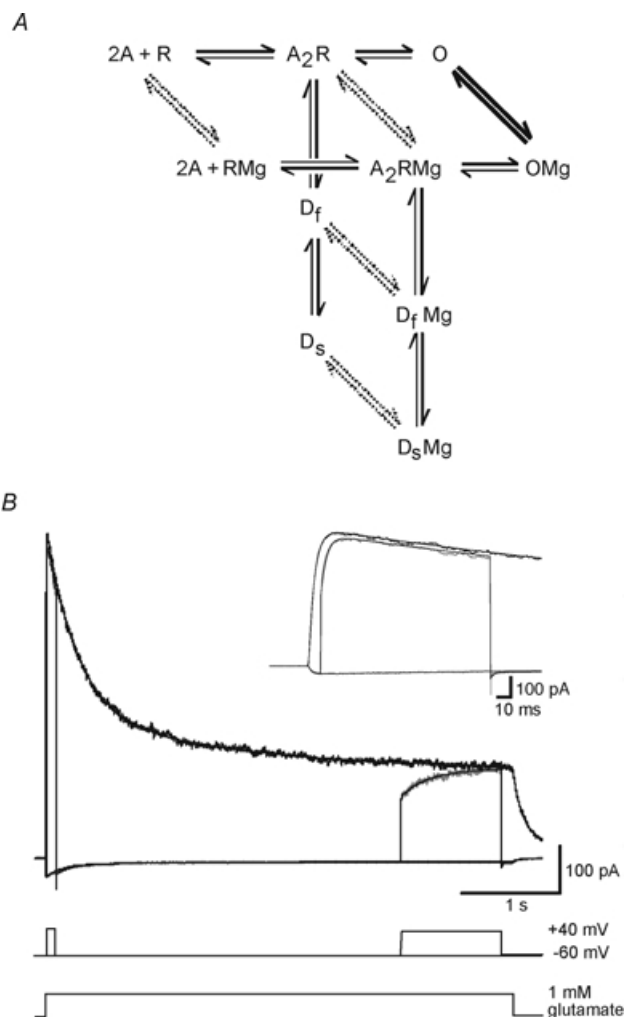


Figure 2. Markov model of NMDAR activation

A, reaction scheme shows two molecules of glutamate (A) binding to the NMDA receptor (R), opening of the channel (O), and transition to fast and slow desensitization states (D_f and D_s). Mg^{2+} binds to all five states, although binding is much more rapid to the open state (thick lines) than to the other states (dashed lines). B, recorded and simulated NMDAR current during 4.6 s applications of 1 mM glutamate in the presence of 1 mM Mg^{2+} at holding potentials of -60 and $+40 \text{ mV}$ (black), and during a step from -60 to $+40 \text{ mV}$ starting 10 ms (see inset with expanded time scale) or 3.5 s after the glutamate application (grey). Fitted transients (smooth curves) generated by the model shown in A are superimposed on the data.

Table 1. Optimum reaction rates for the Markov model of the NMDAR. Average results from 5 patches.

Transition	Forward Rate		Reverse Rate	
	Mg ²⁺ not bound	Mg ²⁺ bound	Mg ²⁺ not bound	Mg ²⁺ bound
Glutamate binding ($\mu\text{M}^{-1}\text{s}^{-1}$)	10 (fixed)	10 (fixed)	5.6 ± 1.0	17.1 ± 2.5
Channel opening (s^{-1})	10 (fixed)	10 (fixed)	273 ± 12	548 ± 60
Fast desensitisation (s^{-1})	2.2 ± 0.2	2.1 ± 0.3	1.6 ± 0.1	0.87 ± 0.14
Slow desensitisation (s^{-1})	0.43 ± 0.09	0.26 ± 0.07	0.50 ± 0.13	0.42 ± 0.30
Mg ²⁺ binding ($\mu\text{M}^{-1}\text{s}^{-1}$)*	0.05 (fixed)		12 800 ± 2 200	

*Binding to the open state at +40 mV. The forward rate of Mg²⁺ binding to the other 4 states was arbitrarily constrained to be 1,000 times slower. Reverse rates were constrained by cyclic reversibility during fitting to data from individual patches.

Table 2. Effect of Mg²⁺ binding on NMDAR properties

Property	Mg ²⁺ not bound	Mg ²⁺ bound
K _d for glutamate (μM)	0.56 ± 0.10	1.71 ± 0.25
Open Probability (%)	3.6 ± 0.2	1.9 ± 0.2
Fast Desensitisation (%)	58 ± 2	71 ± 3

voltage steps from -60 to +40 mV starting 3.5 s after the onset of long (4.6 s) glutamate applications, at a time when the NMDAR current was approximately at steady state (Fig. 1C). The resultant current showed significantly slower Mg²⁺ unblock compared to voltage steps evoked 10 ms after glutamate application (compare C with B in Fig. 1). The ratio between the current evoked at +40 mV and that evoked by stepping from -60 to +40 mV starting 3.5 s after onset of glutamate application was best fitted with three exponentials, with a fast time constant of 0.15 ± 0.04 ms of amplitude $46 \pm 3\%$, and two slower time constants of 4.0 ± 0.4 ms and 322 ± 78 ms with amplitudes of $22 \pm 4\%$ and $32 \pm 6\%$, respectively (Fig. 1D and E; 'late step'; $n = 5$). Interestingly, the main difference in the kinetics during early (10 ms) and late (3.5 s) voltage steps from -60 to +40 mV was a reduction in the amplitude of the fastest time constant and the appearance of a third, very slow time constant, with little change in the amplitude or kinetics of the intermediate time constant (Fig. 1E). Stepping back to -60 mV at the end of pulses to +40 mV blocked the channel (Fig. 1C). The time course of Mg²⁺ block was rapid and could be fitted with a single exponential with a time constant of 0.09 ± 0.003 ms ($n = 5$). Together, these results indicate that Mg²⁺ unblock of NMDARs has a slow component, the magnitude and time course of which is dependent on the timing of depolarizations after the onset of glutamate applications.

A 10-state kinetic model of the NMDAR (Fig. 2A) was used to fit current transients generated by voltage steps from -60 to +40 mV applied at short (10 ms) and long (3.5 s) intervals after the onset of glutamate pulses. The fitted model accurately reproduced the slow recovery from

Mg²⁺ block during steps from -60 to +40 mV at both early and late times (Fig. 2B). The optimized reaction rates were consistent from patch to patch ($n = 5$), and are summarized in Table 1. The rates were used to determine the effect of Mg²⁺ binding on NMDAR channel properties, and indicated that when Mg²⁺ is bound, it reduces the channel's affinity for glutamate (K_d) and open probability, but increases the rate of desensitization (Table 2).

A prediction of this model was that the response to a brief pulse of glutamate in the presence of Mg²⁺ will decay more rapidly at negative potentials. This would be expected primarily due to the reduced affinity for glutamate when Mg²⁺ is bound, but enhanced desensitization will also contribute. This prediction was confirmed experimentally. NMDAR current decay kinetics during brief (1 ms) glutamate applications in the presence of Mg²⁺ were clearly voltage dependent, with NMDAR currents decaying faster at negative holding potentials where Mg²⁺ block is greatest (Fig. 3A). This effect was due to the presence of Mg²⁺ as the decay of NMDAR currents was largely voltage independent in Mg²⁺-free solutions (Fig. 3A). A second prediction of the model was that in the presence of Mg²⁺ more desensitization should be observed at negative holding potentials. Consistent with this, during long (4.6 s) applications of glutamate the steady-state current measured at +40 mV was $33 \pm 2\%$ of the peak current, whereas at -60 mV it was only $22 \pm 6\%$ ($n = 5$, $P < 0.05$). Since glutamate binding is saturated in these experiments, this difference is presumably due to the ability of Mg²⁺ to enhance NMDAR desensitization.

The time dependence of slow Mg²⁺ unblock described here is likely to have important physiological consequences for STDP, as brief depolarizations that occur later in time after release of glutamate would be expected to evoke smaller NMDAR currents than predicted assuming instantaneous Mg²⁺ unblock. Indeed, the integral of NMDAR currents evoked by brief (10 ms) depolarizations to +40 mV at different times after brief (1 ms) glutamate applications was dependent on their

millisecond timing, with the relative magnitude of NMDAR currents (compared to the response at +40 mV) smaller during depolarizations later in time after glutamate application (Fig. 3B). Depolarizations evoked 10 ms after glutamate application reached $82 \pm 1\%$ of the maximum NMDAR current at +40 mV, whereas those evoked 100 ms after glutamate application reached only $47 \pm 2\%$ of the maximum current (Fig. 3B; $n = 6$).

These findings suggest that the time dependence of slow Mg^{2+} unblock will influence the time window for NMDAR activation during STDP induction. To test this, we recorded the dendritic membrane potential during pairing of backpropagating APs with EPSPs at different times. Figure 4A (top) shows two examples at time intervals of 10 and 50 ms. We applied these voltage waveforms to patches together with brief (1 ms) glutamate applications

timed to occur at the onset of the dendritic EPSP. Examples of recorded NMDAR currents are shown in Fig. 4A (middle, black). The predicted NMDAR current assuming instantaneous Mg^{2+} unblock was calculated from the steady-state $I-V$ curve for each patch (Fig. 4A, middle, grey). Recorded (black) and predicted (grey) NMDAR conductance were calculated by dividing recorded and predicted NMDAR currents by the voltage driving force (Fig. 4A, bottom). NMDAR activation, defined as the area around the peak in conductance for each EPSP-AP time interval, was calculated for recorded (black) and predicted (grey) NMDAR conductance (Fig. 4B). The timing curve for NMDAR activation observed experimentally (Fig. 4B, black) was significantly narrower (half-duration 43 ms) than that predicted assuming instantaneous Mg^{2+} unblock of NMDAR channels (half-duration 60 ms; Fig. 4B, grey).

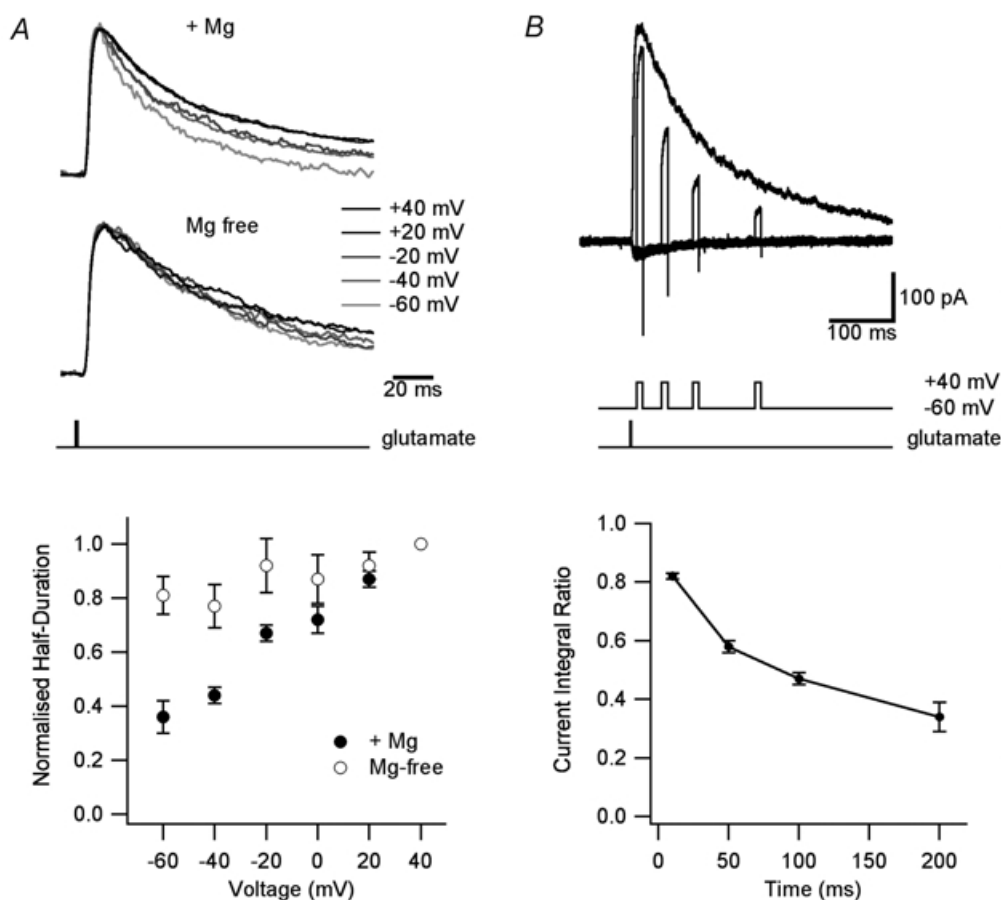


Figure 3. Magnesium affects NMDAR channel activation

A, normalized (at peak), superimposed NMDAR currents during 1 ms applications of 1 mM glutamate at the indicated holding potentials in the presence of 1 mM Mg^{2+} (top) and in Mg^{2+} -free solution (middle). Bottom, average duration at half-amplitude of NMDAR currents evoked by 1 ms applications of 1 mM glutamate normalized to that at +40 mV and plotted against the holding potential in solutions with (●) and without (○) Mg^{2+} ($n = 6$). B, top, superimposed NMDAR currents during 1 ms applications of 1 mM glutamate at +40 mV, and during 10 ms voltage steps from -60 to +40 mV occurring 10, 50, 100 or 200 ms after onset of glutamate application. Bottom, ratio of the current integral during 10 ms voltage steps (as in B) relative to the integral (over the same time) of the response obtained at a holding potential of +40 mV ($n = 6$).

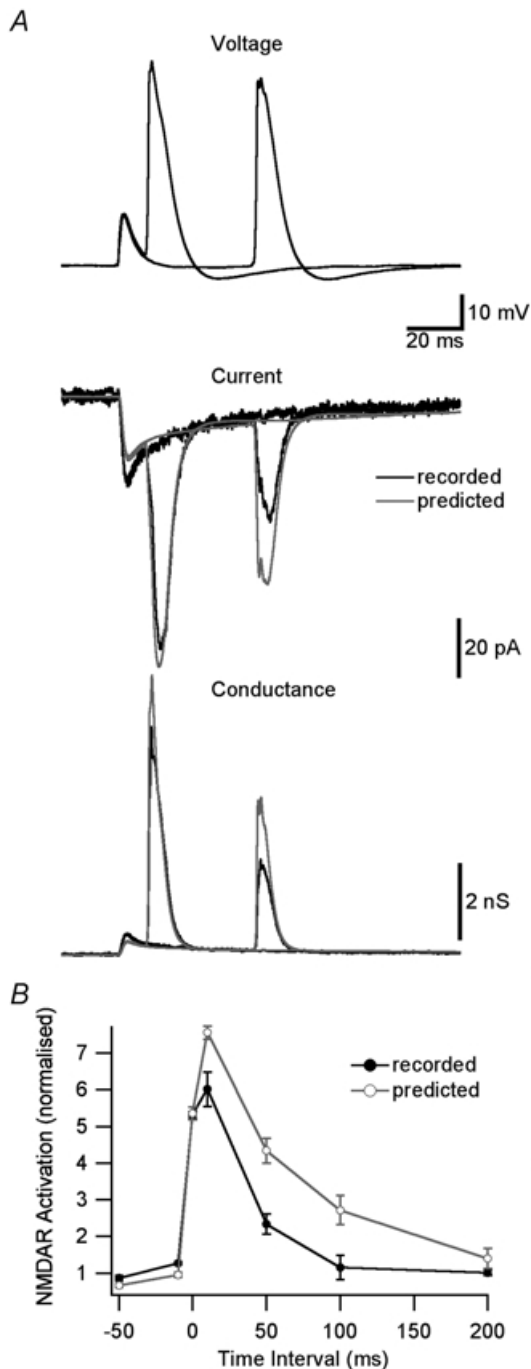


Figure 4. NMDAR activation during STDP induction protocols
 A, top, dendritic voltage (650 μm from the soma) during pairing of an EPSP with a backpropagating AP 10 or 50 ms after EPSP onset. Middle, recorded (black) and predicted (grey, assuming instantaneous Mg²⁺ unblock) NMDAR current during EPSP–AP pairing. Bottom, recorded (black) and predicted (grey) NMDAR conductance. B, NMDAR activation during EPSP–AP pairing at different time intervals for recorded (black) and predicted (grey) NMDAR currents. Currents were normalized in each patch to the response during 1 ms applications of 1 mM glutamate at +40 mV and the area around the conductance peak (3 ms before to 10 ms after) was used to quantify NMDAR activation.

Discussion

Here, we report a slow component to Mg²⁺ unblock of NMDA receptors which has implications for STDP. The kinetics of this slow unblock were dependent on the timing of depolarizations after glutamate application, and were slower during depolarizations at later times. A kinetic model indicated that this occurs due to the ability of Mg²⁺ binding to enhance NMDAR desensitization, while decreasing affinity and open channel probability. Together, these effects act to sharpen the time window during which brief depolarizations, such as backpropagating APs, can activate NMDAR channels.

Comparison with earlier studies

The original studies investigating the kinetics of Mg²⁺ block of NMDARs analysed the dependence of short interruptions in single channel openings on Mg²⁺ concentration and membrane potential (Ascher *et al.* 1988; Jahr & Stevens, 1990*a,b*). These studies estimated that the kinetics of Mg²⁺ block and unblock were fast, with time constants between 80 and 190 μs (Ascher *et al.* 1988; Jahr & Stevens, 1990*a,b*). We find here (see also Spruston *et al.* 1995; Vargas-Caballero & Robinson, 2003) that while the time course of Mg²⁺ block is very fast ($\sim 100 \mu\text{s}$), the time course of Mg²⁺ unblock of NMDARs is complex with a fast component ($\sim 150 \mu\text{s}$) similar to that found in the earlier single channel studies, as well as additional slower components ranging from a few to hundreds of milliseconds depending on the state of the NMDAR channel.

Other studies have reported that Mg²⁺ can be trapped in the NMDAR channel pore, and have proposed a symmetric trapping block model to account for the action of Mg²⁺ on NMDAR channels (Sobolevsky & Yelshansky, 2000). Our model (Fig. 2B) also required Mg²⁺ binding to open, as well as closed and desensitized states, but is not strictly a ‘trapping’ model because Mg²⁺ can unbind when the channel is closed (although at very low rates). Allowing Mg²⁺ to bind and unbind from closed states was considered more realistic than a model where this was not the case, but was not essential to obtain adequate fits to the data (J. Clements, unpublished). Another important difference between our model and that of Sobolevsky & Yelshansky (2000) is that it is asymmetric, with transitions between Mg²⁺-bound states being different from equivalent transitions between Mg²⁺-free states. This asymmetry was essential for adequate fits to the data.

An important conclusion from our study is that Mg²⁺ binding enhances NMDAR desensitization, while

decreasing affinity and open channel probability. This differs from recent data suggesting that Mg^{2+} binding does not affect channel gating, desensitization or agonist dissociation based on the similarity of the IC_{50} for Mg^{2+} block and the K_d for Mg^{2+} binding determined from single channel data (Qian *et al.* 2002). Using the average reaction rates in Table 1, the IC_{50} and K_d for Mg^{2+} block at -60 mV in our kinetic model were $40 \mu M$ and $19 \mu M$, respectively. To detect such a relatively small difference would require an exceptionally accurate dose–response experiment, combined with very high quality single channel recordings from the same preparation. In addition, this previous study examined steady-state Mg^{2+} block where effects of Mg^{2+} binding on desensitization would not be apparent. Consistent with an effect of Mg^{2+} binding on channel gating the extent of desensitization measured by the ratio of the peak to steady-state current during long glutamate pulses, as well as the rate of deactivation during brief glutamate applications, were greater at negative membrane potentials. Finally, these observations are in agreement with the original findings of Nowak *et al.* (1984), who reported that single channel burst duration and frequency are decreased at negative holding potentials where Mg^{2+} binding is greatest.

Consistent with the recent findings of Vargas-Caballero & Robinson (2003), we observed that the slow component of Mg^{2+} unblock accounts for approximately 50% of the amplitude of NMDAR current during depolarizations from -60 to $+40$ mV under steady-state conditions (Fig. 1E, 'late step'). In our hands, slow unblock at these times was better fitted with two exponentials with time constants of approximately 4 and 300 ms rather than one with a time constant of approximately 20 ms. Importantly, we found that the kinetics of slow unblock were faster during depolarizations at earlier times after the onset of glutamate application, with the slow component of Mg^{2+} unblock of NMDARs being best fitted with a single exponential of approximately 4 ms and an amplitude of approximately 25% during depolarizations 10 ms after the onset of glutamate application (Fig. 1E, 'early step').

Mechanism underlying slow unblock

We hypothesize that the slow component to Mg^{2+} unblock described here arises because at negative potentials NMDAR channels go into Mg^{2+} -bound closed and desensitized states, and only slowly re-sensitize and become available to reopen following a step from negative to positive potentials. As the number of NMDAR channels

in Mg^{2+} -bound closed and desensitized states increases with time after the onset of glutamate application, the magnitude and kinetics of Mg^{2+} unblock depend critically on the millisecond timing of depolarizations, with depolarizations occurring early in time after glutamate application leading to larger NMDAR currents due to reduced slow Mg^{2+} unblock (Fig. 3B).

Functional implications

There are a number of potentially important functional implications of our findings. Firstly, we show that enhanced desensitization by Mg^{2+} results in the decay of NMDAR currents being voltage dependent, and faster at negative holding potentials where Mg^{2+} block is greatest (Fig. 3A). This finding is consistent with earlier observations in motoneurons and hippocampal granule cells where the kinetics of NMDAR EPSCs were also found to be voltage-dependent and faster at more negative holding potentials (Konnerth *et al.* 1990; Keller *et al.* 1991). One consequence of this voltage dependence is that synaptic NMDAR currents are prolonged at depolarized membrane potentials, which could enhance NMDAR-dependent calcium influx and synaptic plasticity when presynaptic synaptic activity is paired with postsynaptic depolarization.

Secondly, we show that the magnitude of NMDAR current generated by brief voltage steps or dendritic AP waveforms is dependent on their millisecond timing relative to the onset of glutamate applications (Figs 3B and 4B). This is because Mg^{2+} binding enhances desensitization and reduces glutamate affinity, reducing the relative current flow through NMDARs during brief depolarizations occurring later in time after glutamate application. As the timing of APs relative to EPSP onset plays an important role in determining both the sign and the magnitude of changes in synaptic strength during STDP (Bi & Poo, 1998; Markram *et al.* 1997), the time dependence of slow Mg^{2+} unblock observed here would be expected to sharpen the time window for STDP induction, increasing the ability of the NMDAR channel to function as a coincidence detector.

Finally, slow Mg^{2+} unblock will favour NMDAR activation, and associated calcium influx, during slow dendritic depolarizations, as occurs during dendritic calcium spikes associated with burst firing (Stuart *et al.* 1997) or synaptic stimulation (Schiller *et al.* 1997), increasing the importance of local dendritic regenerative activity near the site of synaptic input for the induction of synaptic plasticity (Golding *et al.* 2002).

References

- Ascher P, Bregestovski P & Nowak L (1988). N-methyl-D-aspartate-activated channels of mouse central neurons in magnesium-free solutions. *J Physiol* **399**, 207–226.
- Bekkers JM & Stevens CF (1989). NMDA and non-NMDA receptors are co-localized at individual excitatory synapses in cultured rat hippocampus. *Nature* **341**, 230–233.
- Bi GQ & Poo MM (1998). Synaptic modifications in cultured hippocampal neurons: dependence on spike timing, synaptic strength, and postsynaptic cell type. *J Neurosci* **18**, 10464–10472.
- Bliss TVP & Collingridge GL (1993). A synaptic model of memory: long-term potentiation in the hippocampus. *Nature* **361**, 31–39.
- Clements JD, Lester RA, Tong G, Jahr CE & Westbrook GL (1992). The time course of glutamate in the synaptic cleft. *Science* **258**, 1498–1501.
- Clements JD & Westbrook GL (1991). Activation kinetics reveal the number of glutamate and glycine binding sites on the N-methyl-D-aspartate receptor. *Neuron* **7**, 605–613.
- Colquhoun D, Jonas P & Sakmann B (1992). Action of brief pulses of glutamate on AMPA/kainate receptors in patches from different neurons of rat hippocampal slices. *J Physiol* **458**, 261–287.
- Forsythe ID & Westbrook GL (1988). Slow excitatory postsynaptic currents mediated by N-methyl-D-aspartate receptors on cultured mouse central neurons. *J Physiol* **396**, 515–533.
- Golding NL, Staff NP & Spruston N (2002). Dendritic spikes as a mechanism for cooperative long-term potentiation. *Nature* **418**, 326–331.
- Jahr CE & Stevens CF (1990a). A quantitative description of NMDA receptor-channel kinetic behavior. *J Neurosci* **10**, 1830–1837.
- Jahr CE & Stevens CF (1990b). Voltage dependence of NMDA-activated macroscopic conductances predicted by single-channel kinetics. *J Neurosci* **10**, 3178–3182.
- Johnson JW & Ascher P (1992). Equilibrium and kinetic study of glycine action on the N-methyl-D-aspartate receptor in cultured mouse brain neurons. *J Physiol* **455**, 339–365.
- Keller BU, Konnerth A & Yaari Y (1991). Patch clamp analysis of excitatory synaptic currents in granule cells of rat hippocampus. *J Physiol* **435**, 275–293.
- Konnerth A, Keller BU, Ballanyi K & Yaari Y (1990). Voltage sensitivity of NMDA-receptor mediated postsynaptic currents. *Exp Brain Res* **81**, 209–212.
- Markram H, Lübke J, Frotscher M & Sakmann B (1997). Regulation of synaptic efficacy by coincidence of postsynaptic APs and EPSPs. *Science* **275**, 213–215.
- Mayer ML, Westbrook GL & Guthrie PB (1984). Voltage-dependent block by Mg²⁺ of NMDA responses in spinal cord neurons. *Nature* **309**, 261–263.
- Nowak L, Bregestovski P, Ascher P, Herbet A & Prochiantz A (1984). Magnesium gates glutamate-activated channels in mouse central neurons. *Nature* **307**, 462–465.
- Qian A, Antonov SM & Johnson JW (2002). Modulation by permeant ions of Mg²⁺ inhibition of NMDA-activated whole-cell currents in rat cortical neurons. *J Physiol* **538**, 65–77.
- Rosenmund C, Feltz A & Westbrook GL (1995). Synaptic NMDA receptor channels have a low open probability. *J Neurosci* **15**, 2788–2795.
- Sather W, Dieudonné S, MacDonald JF & Ascher P (1992). Activation and desensitization of N-methyl-D-aspartate receptors in nucleated outside-out patches from mouse neurons. *J Physiol* **450**, 643–672.
- Schiller J, Schiller Y, Stuart G & Sakmann B (1997). Calcium action potentials restricted to distal apical dendrites of rat neocortical pyramidal neurons. *J Physiol* **505**, 605–616.
- Sobolevsky AI & Yelshansky MV (2000). The trapping block of NMDA receptor channels in acutely isolated rat hippocampal neurons. *J Physiol* **526**, 493–506.
- Spruston N, Jonas P & Sakmann B (1995). Dendritic glutamate receptor channels in rat hippocampal CA3 and CA1 pyramidal neurons. *J Physiol* **482**, 325–352.
- Stuart G, Schiller J & Sakmann B (1997). Action potential initiation and propagation in rat neocortical pyramidal neurons. *J Physiol* **505**, 617–632.
- Vargas-Caballero M & Robinson HP (2003). A slow fraction of Mg²⁺ unblock of NMDA receptors limits their contribution to spike generation in cortical pyramidal neurons. *J Neurophysiol* **89**, 2778–2783.

Acknowledgements

This work was supported by grants from the Alexander von Humboldt Foundation, the National Health and Medical Research Council of Australia (ID 224223), the Australian Research Council (J.D.C.) and a PhD scholarship to B.M.K. from the Australian National University.